ARTICLE NO. 79-1545R

Turbulent Wake of a Thin, Flat Plate

Irwin E. Alber*
Areté Associates, Santa Monica, Calif.

An analytical solution is developed in two near-wake regions using an inner and outer layer coordinate expansion technique. In region I, extending downstream approximately ten initial sublayer thicknesses, a laminar inner wake grows into the trailing-edge laminar sublayer yielding the Goldstein solution, where the centerline velocity and inner thickness grow as $x^{1/3}$. In region II, extending downstream approximately ten full boundary-layer thicknesses, a turbulent inner layer grows into the initial logarithmic layer; here the centerline velocity is shown to increase logarithmically with downstream distance. Comparisons of the solution are made with the near-wake data of Chevray and Kovasznay.

Nomenclature

B	= law-of-the-wall constant = 5.0
C_D	= flat plate drag coefficient
$E_1(\eta), E_i(\eta)$	= exponential integrals
$f(\eta)$	= stream function similarity variable (region I)
$F'(\eta)$	= velocity similarity variable (region II)
$g(x)$	= length variable, nondimensional (region II)
ℓ	= Prandtl mixing length
L	= plate length
P	= static pressure
R	= Reynolds number based on plate length
u^*, v^*	= mean velocities, physical variables, along and normal to wake axis
u, v	= nondimensional velocities, u^*/u_τ, v^*/u_τ
u_τ	= friction velocity, (τ_w/ρ)
$-\overline{u'v'}$	= turbulent Reynolds stress divided by ρ
x^*, y^*	= physical distance along and normal to wake axis
x, y	= nondimensional distance, e.g., $x^* u_\tau/\nu$
z_0	= roughness height
δ	= wake or boundary-layer thickness
δ_s	= inner layer thickness
ϵ	= turbulent eddy diffusivity
η	= similarity variable $y/3x^{1/3}$ (region I) and $y/g(x)$ (region II)
κ	= Karman's constant = 0.41
ν	= kinematic laminar viscosity
ρ	= fluid density
τ_w	= wall shear stress
θ	= trailing-edge momentum thickness

Subscripts

∞	= freestream
$\mathfrak{L}$	= centerline
PG	= pressure gradient

Superscripts

$(\,)'$	= differentiation of $f(\eta)$ with respect to η or fluctuating component of velocity

Presented as Paper 79-1545 at the AIAA 12th Fluid and Plasma Dynamics Conference, Williamsburg, Va., July 23-25, 1979; submitted June 25, 1979; revision received Jan. 10, 1980.

Index category: Jets, Wakes, and Viscid-Inviscid Flow Interactions.

*Senior Scientist. Member AIAA.

I. Introduction

CALCULATION of the viscous wake immediately downstream of the trailing edge of a thin flat plate represents not only a classical problem in fluid mechanics but an important aerodynamics problem related to the prediction of lift and drag on thin airfoils. For most engineering applications, the Reynolds number, based on plate length, is large enough for the trailing-edge boundary layer to be considered fully turbulent. Analytical solutions for the wake downstream of the trailing edge (pioneered by Goldstein[1]) have been obtained primarily for the case of a laminar initial boundary layer with laminar viscous stresses in the near wake. While various numerical treatments exist for the equivalent turbulent problem (e.g., Bradshaw,[2] NASA Free Turbulent Shear Flow Conference,[3] Burgraff[4]), no comprehensive turbulent mathematical analysis exists which corresponds to Goldstein's treatment of the laminar near wake.

The development of the corresponding turbulent near-wake analysis is the subject of this paper. Emphasis will be placed on two inner regions near the trailing edge shown in Fig. 1. Basically, region I is the laminar growth of the inner wake layer into the laminar sublayer. Region II is the turbulent growth of the inner wake into the remnant of the initial wall logarithmic layer. The outer wake layer for these two regions represents, as will be shown, the convected remnant of the upstream boundary layer responding slowly to the changed boundary conditions transmitted to it by the inner wake.

In the turbulent near-wake problem posed here, the initial boundary layer is assumed to be an equilibrium constant pressure turbulent boundary layer. For this boundary layer, as in Goldstein's laminar case, we can distinguish a very small region near the wall where the mean velocity is linear in the vertical dimension y^*. Based on the usual law-of-the-wall scaling for the laminar sublayer, we can describe the initial laminar sublayer mean velocity profile (at the trailing edge) by the linear relationship

$$\frac{u^*}{u_\tau} = \frac{y^* u_\tau}{\nu} \qquad \text{(laminar sublayer)} \qquad (1)$$

This linear profile is approximately valid in the region close to the wall where $y^* u_\tau/\nu < 11$-20.

In the laminar sublayer region of the initial boundary layer, the turbulent Reynolds stresses are assumed to be small compared to the laminar viscous stresses. If we adopt an eddy viscosity model for the turbulent Reynolds stresses, i.e., $-\overline{u'v'} = \epsilon \partial u^*/\partial y^*$, then $\epsilon/\nu \ll 1$ in the sublayer region. Because of the presence of the linear sublayer velocity profile near the wall at the trailing edge, we can expect, for a short distance just downstream of the trailing edge, that a laminar "inner" wake should develop which behaves like the inner

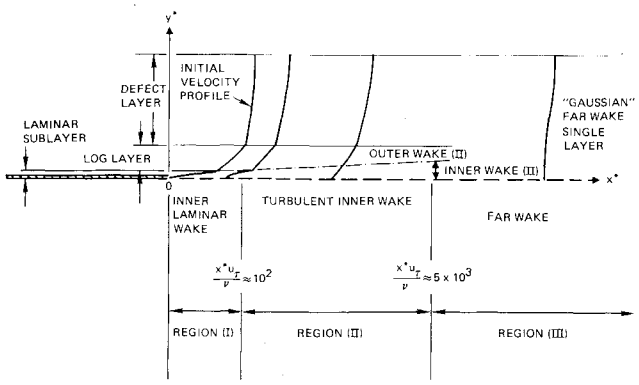

Fig. 1 Near- and far-wake regions; turbulent wake of a flat plate.

laminar Goldstein solution. As we will show in Sec. II of this paper, the initial inner wake solution (region I) will be of the Goldstein form (written in "wall" variables)

$$u^*/u_\tau = (x^*u_\tau/\nu)^{1/3} f_0'(\eta) \tag{2}$$

Asymptotically, for large η, the similarity function $f_0'(\eta)$ behaves as

$$f_0'(\eta) \sim \eta \qquad \eta \to \infty$$

with

$$\eta = \frac{1}{3}\left(\frac{y^*u_\tau}{\nu}\right) \Big/ \left(\frac{x^*u_\tau}{\nu}\right)^{1/3} \tag{3}$$

Note that the thickness of the laminar inner wake increases with axial distance to the one-third power. The linear velocity profile outer boundary condition will be approximately valid only as long as the thickness of the inner wake layer does not exceed the height of the initial laminar sublayer, i.e., $\delta_s u_\tau/\nu < 11\text{-}20$. Thus Eq. (3) implies that the region for "laminar-like" wake development, referred to as region I, will be small—in the range $0 < (x^*u_\tau/\nu) < 50\text{-}400$. Over this downstream distance, the centerline axial velocity will have increased rapidly from zero to about $u_\ell^*/u_\tau = 6\text{-}12$, i.e., to $u_\ell^*/u_\infty^* = 0.24\text{-}0.48$. Thus the centerline velocity will have increased to a substantial fraction of the freestream velocity in an axial distance of only about 0.1 to 0.4 initial boundary-layer thicknesses ($R_\delta = 1.5 \times 10^4$).

Downstream of the point where the inner wake has "consumed" the laminar sublayer, the inner wake will next being to "eat" into the logarithmic remnant of the trailing edge boundary layer. This portion of the x^* axis is called region II (see Fig. 1).

In the logarithmic or law-of-the-wall part of the initial turbulent boundary layer, the mean velocity profile can be described by the well-known expression[5]:

$$\frac{u^*}{u_\tau} = \frac{1}{\kappa} \ell n \frac{y^*u_\tau}{\nu} + B \qquad \text{(logarithmic region)} \tag{4}$$

where κ is Karman's constant $= 0.41$ and $B = 5.0$.

In the logarithmic layer upstream of the trailing edge, the Reynolds stress is nearly constant and the turbulent eddy diffusivity is assumed much larger than the laminar diffusivity $\epsilon/\nu \gg 1$. In the logarithmic layer, the eddy diffusivity increases linearly with distance from the wall according to

$$\epsilon = \kappa u_\tau y^* \quad \text{(logarithmic layer)} \tag{5}$$

To simplify the analysis for the region II inner wake development, we assume that the linear eddy diffusivity relation [Eq. (5)] is also valid in the near wake and holds all the way down to the wake axis (i.e., $\epsilon = \kappa u_\tau |y^*|$). Thus we ignore a region extremely close to the axis where ϵ may level off at a small constant value. Other more complex models may be utilized, e.g., Bradshaw,[2] but the simplicity of the present treatment is lost.

The scaling for the region II inner wake (given in Sec. III) is developed along lines similar to that used by Townsend[8,9] for the problem of the adjustment of a turbulent boundary layer to a sudden change in surface roughness. Townsend showed that after a step change in surface roughness, an inner layer (with similarity or self-preserving structure) develops within an initial logarithmic outer layer. He showed that the scale height δ_s of the inner layer is determined by the expression

$$\delta_s \left(\ell n \frac{\delta_s}{z_0} - 1\right) = 2\kappa^2 x^* \tag{6}$$

where z_0 is the local surface roughness height. Equation (6) is valid provided that $\ell n(\delta_s/z_0)$ is large and the change in friction velocity is also large.

In the analysis for the region II wake, the characteristic upstream length scale is ν/u_τ. The growth of the inner layer for a region II similarity solution will be shown to be given by an analogous expression with ν/u_τ replacing z_0.

The corresponding centerline velocity for such an inner wake will subsequently be shown in Sec. III to be of the form

$$\frac{u^*}{u_\tau} = \frac{1}{\kappa}[\ell n g(x) + F'(y^*/\delta_s)] \tag{7}$$

where $g(x)$ and $\delta_s(x)$ are determined by the similarity requirements imposed by Eq. (7) on the equations of motion.

As brought to this author's attention[6] after a first draft of this paper had been written, a similarity solution for turbulent inner wake growth in region II was, in fact, first developed by Robinson[7] in 1967 as part of an NPL report. Assuming self-preserving forms for the terms in Townsend's kinetic energy equation, Robinson correctly derived the logarithmic increase of centerline velocity for region II as indicated by Eq. (7). Robinson, however, was not able to verify the logarithmic wake velocity behavior by making comparisons with detailed wake velocity data.

In this paper, the region II inner wake solution will be shown to be a valid similarity solution when developed according to a series expansion for $F'(\eta)$, valid when $\ell n(\delta_s u_\tau/\nu) \gg 1$. Note that the logarithmic term in x given in Eq. (7) is readily suggested by the asymptotic requirement that $(u/u_\tau)_{\text{inner}} \to (1/\kappa)\ell n(y^*u_\tau/\nu) + B$, as $(y^*u_\tau/\nu)_{\text{inner}} \to \infty$. Thus, the inner wake will show a slow logarithmic increase in the centerline velocity in region II, following the initial rapid rise which occurs in region I. It should be added that the "outer" layer in region II will be perturbed by the negative vertical velocity induced by the acceleration of the inner wake. The basic form of the outer solution will be given at the conclusion of Sec. III.

Comparisons of the wake velocity field solution with the mean velocity near-wake data of Chevray and Kovasznay[10] will be presented in Sec. IV. As will be shown, these comparisons validate the logarithmic growth of wake centerline velocity for region II. Hence, the scaling of near-wake centerline data using the far-wake formula $(u_\infty^* - u_\ell^*)/u_\infty^* \sim (x^*/C_D L)^{-1/2}$ will be shown to be incorrect for distances less than approximately ten boundary-layer thicknesses from the trailing edge.

Finally, as in the triple-deck analysis of Stewartson[11] and Messiter,[12] we note that the near-wake analysis must be formally corrected to allow for viscous-inviscid interactions near the trailing edge (induced pressure gradients) in order to avoid singularities in the inner wake vertical velocity component at the trailing edge. Further steps are required to modify the present turbulent wake analysis in order to allow for the effects of induced pressure gradients. These "triple

deck'' modifications are briefly discussed at the conclusion of this paper. We find that the scaling for such interactions follows the work of Lighthill[13] on interacting compressible boundary layers.

II. Laminar Sublayer Near Wake (Region I)

Goldstein's[1] coordinate expansion solution for the inner and outer laminar wake layers can be applied directly to the problem of the initial region of turbulent wake development (region I), where laminar diffusion dominates near the axis. For distances $x^*u_\tau/\nu \leq 0(10^2)$, the inner wake layer grows into the laminar sublayer of the initial boundary layer.

The variables appearing in the Reynolds' averaged boundary-layer equations are written in ''law-of-the-wall'' coordinates in order to readily introduce the initial turbulent boundary-layer velocity profile in its ''law-of-the-wall'' format. Nondimensional variables are defined by

$$x=x^*u_\tau/\nu, \quad y=y^*u_\tau/\nu, \quad u=u^*/u_\tau, \quad v=v^*/u_\tau$$

The origin of the coordinate system is taken to be the trailing edge of the flat plate, with x along the axis of the two-dimensional wake in the freestream direction, and y normal to it.

Using an eddy diffusivity representation for the Reynolds stress term $-\overline{u'v'}$, we have the following nondimensional forms for the continuity and axial momentum equations (assuming zero pressure gradient in the wake $dP/dx=0$)

$$\frac{\partial u}{\partial x}+\frac{\partial v}{\partial y}=0 \tag{8}$$

$$u\frac{\partial u}{\partial x}+v\frac{\partial u}{\partial y}=\frac{\partial}{\partial y}\left[\left(1+\frac{\epsilon}{\nu}\right)\frac{\partial u}{\partial y}\right] \tag{9}$$

For the laminar sublayer wake development in region I, we assume that $\epsilon_{\text{wake}}/\nu \ll 1$. Hence, Eq. (9) can be written in the laminar boundary-layer form

$$u\frac{\partial u}{\partial x}+v\frac{\partial u}{\partial y}=\frac{\partial^2 u}{\partial y^2} \quad \text{(region I)} \tag{10}$$

The boundary and initial conditions are:

$$\frac{\partial u}{\partial y}=v=0 \quad \text{for } x>0,\ y=0 \tag{11}$$

$$u(0,y)=y \quad \text{for } y>0,\ x=0 \tag{12}$$

Note that we have neglected additional higher-order terms in the Taylor's series expansion for $u(0,y)$.

The first term in the Goldstein power series expansion for the inner wake thus constitutes the similarity solution for the region I development, i.e.,

$$u=\frac{1}{3}x^{1/3}f'(\eta) \tag{13}$$

For the continuity equation, Eq. (8), the normal velocity is

$$v=-\frac{1}{3}x^{1/3}[2f-\eta f'] \tag{14}$$

The similarity variable η is given by

$$\eta=\frac{1}{3}(y/x^{1/3}) \tag{15}$$

and primes denote differentiation with respect to η. Substituting Eqs. (13) and (14) into the momentum equation, Eq. (10), yields Goldstein's nonlinear ordinary differential equation for $f(\eta)$

$$f'^2-2ff''-f''=0 \tag{16}$$

$$f(0)=f''(0)=0 \tag{17}$$

The linear form of the initial velocity profile, $u=u(0,y)=y$, sets the outer boundary condition for $f(\eta)$. For $x\to 0$, with η fixed,

$$f'(\eta)\to 9\eta \quad \text{as } \eta\to\infty \tag{18}$$

For small η, Goldstein developed the following power series expansion for $f'(\eta)$

$$f'(\eta)=\beta_0+\beta_0^2\frac{\eta^2}{2!}-2\beta_0^3\frac{\eta^4}{4!}+\ldots \tag{19}$$

The axis velocity constant β_0 is determined by the asymptotic form for $f'(\eta)$ according to

$$\beta_0=[\lim_{\eta\to\infty}(f'(\eta)/\eta)/\lim_{\eta\to\infty}F_0''(\eta)]^{2/3} \tag{20}$$

where $F_0'(\beta_0^{1/2}\eta)\equiv f'(\eta)$ and F_0' satisfies Eqs. (16) and (17) with the axis boundary condition $F_0'(0)=1$.

Using the numerical value given by Goldstein, $\lim_{\eta\to\infty} F_0''=\gamma_0=0.84712$, and the constant of proportionality given in Eq. (18), one finds that $\beta_0=4.8328$. Hence the centerline velocity, according to Eqs. (13) and (19), is

$$u(x,0)=1.61093x^{1/3} \quad x>0 \tag{21}$$

The wake centerline velocity in terms of physical coordinates and parameters can then be rewritten as

$$u_\ell^*/u_\tau=1.61093(x^*u_\tau/\nu)^{1/3} \tag{22}$$

For large η, Goldstein found numerically that the asymptotic form of the similarity solution included a constant of integration such that

$$\lim_{\eta\to\infty}F_0'(\beta_0^{1/2}\eta)\to\gamma_0(\beta_0^{1/2}\eta+\delta_0) \tag{23}$$

with

$$\gamma_0=\frac{9}{\beta_0^{3/2}}=0.84712, \quad \delta_0=0.65364 \tag{24}$$

Hence the limiting solution for u at large y is:

$$\lim_{y\to\infty}u\to y+\frac{1}{3}\beta_0\gamma_0\delta_0x^{1/3}=y+0.89199x^{1/3} \tag{25}$$

The corresponding asymptotic form for the vertical velocity component v is

$$\lim_{y\to\infty}v\sim-\frac{1}{3}x^{1/3}[\gamma_0\delta_0\beta_0\eta+\beta_0^{1/2}\gamma_0\delta_0^2] \tag{26}$$

$$\lim_{y\to\infty}v\sim-\frac{1}{9}x^{-2/3}[\gamma_0\delta_0\beta_0]y-\frac{\beta_0^{1/2}\gamma_0\delta_0^2}{3}x^{-1/3} \tag{27}$$

For large y, v is then given by

$$v\sim-0.2973x^{-2/3}y \tag{28}$$

The asymptotic character of the inner layer solution motivated the form of Goldstein's expansion solution for the outer layer. In our turbulent case, the scale of the outer layer

is of order $y^*/L \approx O(\delta/L) \sim O(u_\tau/u_\infty)$. Following Goldstein's expansion procedure, the corresponding leading term in the outer layer solution for small x would be [from Eqs. (25) and (28)]

$$u_{\text{outer}} = u(0,y) + A(x)\frac{\mathrm{d}}{\mathrm{d}y}[u(0,y)] \tag{29}$$

$$v_{\text{outer}} = -A'(x)u(0,y) \tag{30}$$

where, matching with the inner solution, we find that

$$A(x) = \frac{1}{3}\beta_0\gamma_0\delta_0 x^{1/3} \tag{31}$$

The outer velocities, given by Eqs. (29) and (30), correspond to a solution of the inviscid equations of motion for the outer layer (i.e., all viscous terms are ignored). The function $A(x)$ represents simply the displacement effect correction to the outer flow induced by the acceleration of the inner layer.

The inner and outer solutions, represented by Eqs. (13), (14), and (29-31), are of course only valid in wake region I over a short distance downstream of the trailing edge of the flat plate, of the order of 10-100 initial laminar sublayer thicknesses. The theory for the wake development in region II, downstream of the rapid laminar acceleration of region I, is given next.

III. Turbulent Logarithmic Near Wake (Region II)

The solution in region II ($10^2 < x^* u_\tau/\nu < 10^4$) treats a portion of the near wake where it is assumed that the turbulent velocity and length scales are still of the same order as in the logarithmic portion of the trailing-edge boundary layer [$\sqrt{\overline{u'^2}} = O(u_\tau)$, $\ell \sim O(y)$]. The diffusion process is assumed dominated by turbulent, rather than laminar, mixing (i.e., $\epsilon/\nu \gg 1$). Using the linear form for the eddy diffusivity [Eq. (5)], the normalized momentum equation for the wake ($y \geq 0$) is given by

$$u\frac{\partial u}{\partial x} + v\frac{\partial u}{\partial y} = \frac{\partial}{\partial y}\left[\kappa y \frac{\partial u}{\partial y}\right] \tag{32}$$

We seek a solution of Eq. (32) and the continuity equation [Eq. (8)] which is valid for large x such that, for a fixed value of x,

$$\lim_{y\to\infty} u \sim (1/\kappa)\ln y + B \tag{33}$$

A. Similarity Solution for Region II

Equation (33) suggests a solution of the form

$$u = S(x) + (1/\kappa)F'(\eta) \tag{34}$$

where $\eta = y/g(x)$ and primes denote differentiation with respect to η or x. From the continuity equation,

$$v = -S'\eta g + g'(\eta F' - F)/\kappa \tag{35}$$

Substituting for u and v into the momentum equation [Eq. (32)] and collecting the dominant terms on the left-hand side of Eq. (36) yields

$$[F''\eta]' + \frac{g'S}{\kappa}[F''\eta] - gSS' = \frac{gS'}{\kappa}[F' - \eta F''] - \frac{g'}{\kappa}FF'' \tag{36}$$

To obtain a similarity solution for F (for large x or g), we must set the two functions of x, appearing as coefficients on the right-hand side of Eq. (36), equal to constants. Without loss of generality, we can write

$$g'S/\kappa = 1, \quad gSS' = 1 \tag{37}$$

Thus, upon integrating Eq. (37), we find that the two x-dependent functions S and g satisfy

$$S(x) = (1/\kappa)\ln g(x) \tag{38}$$

and

$$g(x)[\ln g(x) - 1] = \kappa^2 x \tag{39}$$

Note that in Eq. (39) there is some arbitrariness in the origin of x. For convenience we set the origin at x equal to zero, which corresponds to the condition $g = e^1$.

Using Eqs. (38) and (39), the momentum equation [Eq. (36)] is then rewritten as

$$[F''\eta]' + [F''\eta] - 1 = \frac{1}{\ln g}[F' - \eta F'' - FF''] \tag{40}$$

When $\ln g$ is large $F(\eta)$ can be expanded in series as

$$F = F_0(\eta) + \frac{1}{\ln g}F_1(\eta) + \frac{1}{(\ln g)^2}F_2(\eta) + \ldots \tag{41}$$

i.e., when $1/\ln g \ll 1$.

Thus, from Eq. (40) we see that $F_0(\eta)$ satisfies the linear equation

$$[F_0''\eta]' + [F_0''\eta] - 1 = 0 \tag{42}$$

and F_1 satisfies

$$[F_1''\eta]' + [F_1''\eta] = F_0' - \eta F_0'' - F_0 F_0'' \tag{43}$$

Similar linear equations can be written for all the other higher-order similarly functions, $F_2(\eta)$, etc.

The boundary conditions for $F_0(\eta)$ at the axis are given by the requirement that $v = 0$ on $y = 0$ and that $\partial u/\partial y$ is bounded as $y \to 0$. Thus the centerline conditions are:

$$F_0(0) = 0 \text{ and } \lim_{\eta\to 0^+} \eta F_0''(\eta) = 0 \tag{44}$$

To satisfy the boundary condition for large y (at fixed x), given by Eq. (33), we require that

$$\lim_{\eta\to\infty} F_0' \to \ln\eta + B\kappa \tag{45}$$

The boundary conditions for $F_1(\eta)$ are

$$F_1(0) = 0, \quad \lim_{\eta\to 0^+} \eta F_1''(\eta) = 0, \quad \lim_{\eta\to\infty} F_1'(\eta) = 0 \tag{46}$$

B. Integration of Similarity Equation for $F_0(\eta)$

To solve Eq. (42), subject to boundary conditions (44) and (45), we first integrate the linear equation over η to obtain

$$F_0'' = (1 - e^{-\eta})/\eta \tag{47}$$

Upon integrating, once more we find that

$$F_0' = F_0'(0) + \int_0^\eta \left[\frac{1 - e^{-t}}{t}\right]\mathrm{d}t \tag{48}$$

We can express the velocity profile function $F_0'(\eta)$ in terms of the exponential integral, i.e.,

$$F_0' = F_0'(0) + \gamma + \ln\eta + E_1(\eta) \tag{49}$$

where

$$E_1(\eta) \equiv \int_{\eta}^{\infty} \frac{e^{-t}}{t}\,dt \tag{50}$$

and γ is Euler's constant = 0.5772157.

The value of the similarity velocity constant at the axis $F_0'(0)$ is determined by the asymptotic boundary condition, Eq. (45).

From Eq. (49),

$$\lim_{\eta\to\infty} F_0'(\eta) \sim F_0'(0) + \gamma + \ell n\eta + \frac{e^{-\eta}}{\eta}\left[1 - \frac{1}{\eta} + \frac{2}{\eta^2} - \ldots\right] \sim \ell n\eta + B\kappa \tag{51}$$

Thus we find that

$$F_0'(0) = B\kappa - \gamma \tag{52}$$

This yields the first approximation for the wake centerline velocity in region II, which when written in physical variables, is:

$$\frac{u_{\xi}^*}{u_\tau} = \frac{1}{\kappa}[\ell ng(x) - \gamma] + B \tag{53}$$

Rewriting Eq. (49) using Eq. (52), we have

$$F_0'(\eta) = \ell n\eta + E_1(\eta) + B\kappa \tag{54}$$

A graph of $F_0'(\eta)$ is shown in Fig. 2. Note the finite slope of F_0' at $\eta = 0$, and the asymptotic logarithmic form as $\eta \to \infty$.

Upon integrating Eq. (54) once more with respect to η, we obtain (with $F_0(0) = 0$)

$$F_0(\eta) = \eta[\ell n\eta + E_1(\eta) + B\kappa - 1] + (1 - e^{-\eta}) \tag{55}$$

C. Solution for $F_1(\eta)$

Using the expression for $F_0(\eta)$ and its derivatives given above, we readily find a first integral of Eq. (43):

$$F_1'' = F_0(\eta)\frac{e^{-\eta}}{\eta} + [E_1(\eta) - Ei(\eta) + 2(\ell n\eta + \gamma)]\frac{e^{-\eta}}{\eta} \tag{56}$$

where

$$Ei(\eta) \equiv -\int_{-\eta}^{\infty} \frac{e^{-t}}{t}\,dt \tag{57}$$

is another form of the exponential integral.

Integration of Eq. (56) is not readily expressible in terms of simple tabulated forms of the exponential integral. A numerical integration of Eq. (56) for $F_1'(\eta)$ was performed and the result is shown in the lower curve of Fig. 2. The constant of integration $F_1'(0)$ is again determined by the asymptotic form for F_1', which requires that F_1' vanish for large η.

For large values of η, the dominant term in Eq. (56) contains $Ei(\eta)$. Since

$$\lim_{\eta\to\infty} Ei(\eta) \sim e^{\eta}/\eta \tag{58}$$

then F_1' has the slowly diminishing asymptotic form

$$\lim_{\eta\to\infty} F_1'(\eta) \sim 1/\eta \tag{59}$$

and by integration

$$\lim_{\eta\to\infty} F_1(\eta) \sim \ell n\eta + C \tag{60}$$

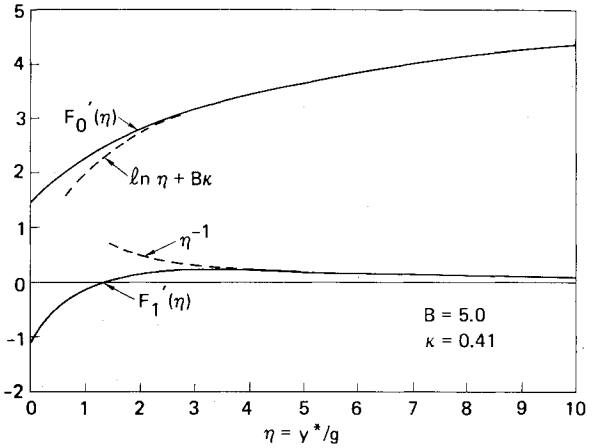

Fig. 2 Velocity profile functions; $F_0'(\eta)$ and $F_1'(\eta)$, $B = 5.0$, $\kappa = 0.41$.

From the numerical solution (evaluated at $\eta = 10$), we find for the constants of integration

$$F_1'(0) = -0.992341, \quad C = -1.343 \tag{61}$$

using $B = 5.0$ and $\kappa = 0.41$.

D. Outer Solution

To determine the leading order perturbation to the outer initial boundary-layer profile $u(0,y)$, we use the asymptotic forms of the inner layer solution as a guide.

For the axial velocity, the first two terms in the series, given by Eq. (41), yield

$$u = \frac{1}{\kappa}\left[\ell ng(x) + F_0'(\eta) + \frac{1}{\ell ng}F_1'(\eta)\right] \tag{62}$$

Using the asymptotic forms, Eqs. (51) and (59), for large values of η,

$$\lim_{\eta\to\infty} u = \frac{1}{\kappa}\left[\ell ng(x) + \ell n\eta + B\kappa + \frac{1}{\eta\ell ng}\right] \tag{63}$$

$$\lim_{\eta\to\infty} u = \frac{1}{\kappa}\ell ny + B + \frac{g}{\ell ng}\left(\frac{1}{\kappa y}\right) \tag{64}$$

The logarithmic and constant terms in Eq. (64) represent the lower limit of the outer initial velocity profile $\lim_{y^*/\delta\to 0} u(x = 0,y)$, and the third term represents the derivative of the initial u velocity profile for small y^*/δ. Thus we can express the leading terms in the outer solution for $u_{\text{outer}}(x,y)$ as

$$u_{\text{outer}}(x,y) = u(0,y) + A(x)\frac{\mathrm{d}}{\mathrm{d}y}[u(0,y)] \tag{65}$$

where $A(x) = g/(\ell ng)$.

For the asymptotic vertical velocity v, we have

$$\lim_{\eta\to\infty} v = \lim_{\eta\to\infty} \frac{\kappa}{\ell ng}\left[\eta\left(F_0' + \frac{1}{\ell ng}F_1' - 1\right) - \left(F_0 + \frac{1}{\ell ng}F_1\right)\right] \sim \frac{-\kappa}{(\ell ng)}[\ell ny + B + \kappa C_2] \tag{66}$$

where $C_2 = C - 1 - B\kappa$.

Following the argument used in deriving the outer form for u in Eq. (65), we can write

$$v_{\text{outer}} = -\left(\frac{\kappa}{\ell ng}\right)^2[u(0,y) + C_2] \tag{67}$$

For large values of y,

$$v_{\text{outer}} \sim -\left(\frac{\kappa}{\ell ng}\right)^2 u(0,y) \tag{68}$$

Note that the derivative with respect to x of the velocity gradient coefficient $A(x)$ appearing in Eq. (65) is:

$$A'(x) = \left(\frac{\kappa}{\ell ng}\right)^2 \left[1 - \frac{1}{\ell ng}\right] \tag{69}$$

For large values of ℓng, we can write

$$v_{\text{outer}} = -A'(x)u(0,y) \tag{70}$$

Thus the region II outer solutions for u and v are coupled in the same fashion as the leading terms of the corresponding Goldstein solution for region I [Eqs. (29) and (30)] with different expressions for $A'(x)$.

IV. Comparisons with Turbulent Wake Data

Chevray and Kovasznay[10] made detailed hot-wire measurements of the mean and fluctuating velocity field in the near wake of a two-dimensional thin flat plate (length = 240 cm, width = 50 cm). The characteristics of their trailing-edge turbulent boundary layer were: Reynolds number based on boundary-layer thickness $Re_\delta = 1.5 \times 10^4$ ($\delta = 5.5$ cm at $u/u_\infty = 0.99$), and Reynolds number based on momentum thickness $Re_\theta = 1.6 \times 10^3$ ($\theta = 0.58$ cm). The wall friction velocity was estimated to be in the range $0.037 < u_\tau/u_\infty < 0.047$.

The measured initial velocity profile at $x = 0$ is plotted in the semilogarithmic "law-of-the-wall" format in Fig. 3. The best fit to the data by the logarithmic formula, Eq. (4) with $B = 5.0$ and $\kappa = 0.41$, yields a value for the trailing-edge friction velocity $u_\tau/u_\infty = 0.043$. This velocity scale factor is used in all subsequent comparisons with the wake data of Chevray and Kovasznay.[10]

Chevray and Kovasznay note two features of their experimental results which lend credence to the assumptions made in the present analytical model of the trailing edge wake problem. First, they state that "Leaving the trailing edge... only the center portion of the flow changes and the outer portion remains the same as the original boundary layer." This statement supports the concept of an inner layer growing inside a nearly constant outer layer. Second, they note that, although pressure measurements were not made (because of very low dynamic pressures), "the constancy of the (wake) momentum thickness in the downstream direction, clearly indicates the absence of any significant pressure gradient." The pressure gradient dP/dx is, as previously stated, assumed negligible in the present version of the near-wake analysis.

A comparison of the first-order solution for the inner wake mean velocity with the wake data of Chevray and Kovasznay is shown in Fig. 3. The first-order inner wake mean velocity profile [from Eqs. (34), (38), and (54)] is given by

$$\frac{u^*}{u_\tau} = \frac{1}{\kappa}\left[\ell ng\left(\frac{x^* u_\tau}{\nu}\right) + \ell n\eta + E_1(\eta)\right] + B$$

or

$$\frac{u^*}{u_\tau} = \frac{1}{\kappa}\ell n\left(\frac{y^* u_\tau}{\nu}\right) + B + \frac{1}{\kappa}E_1(y/g(x)) \tag{71}$$

where $g(x)$ is given by Eq. (39).

Relatively good agreement between the theory and the measured inner wake velocity profiles is seen in the region $y^* u_\tau/\nu < 200$. Equation (71), of course, does not treat Coles' "law of the wake" region for $y^* u_\tau/\nu > 200$.

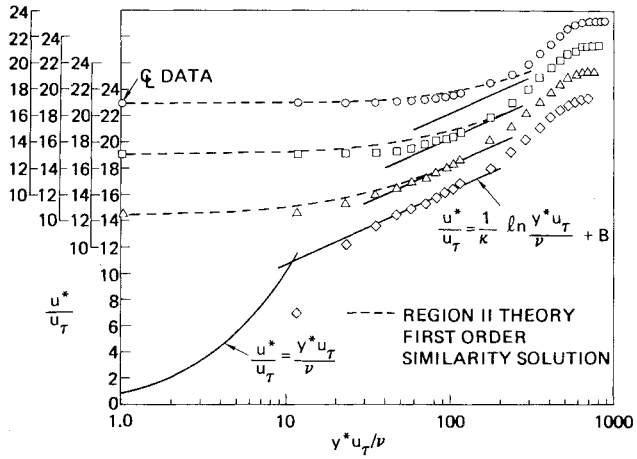

Fig. 3 Near-wake velocity profiles in law-of-the-wall coordinates. Data of Chevray and Kovasznay[10]: ◇ $x^* = x^* u_\tau/\nu = 0$; △ $x^* = 5$ cm, $x^* u_\tau/\nu = 586$; □ $x^* = 20$ cm, $x^* u_\tau/\nu = 2342$; ○ $x^* = 50$ cm, $x^* u_\tau/\nu = 5855$.

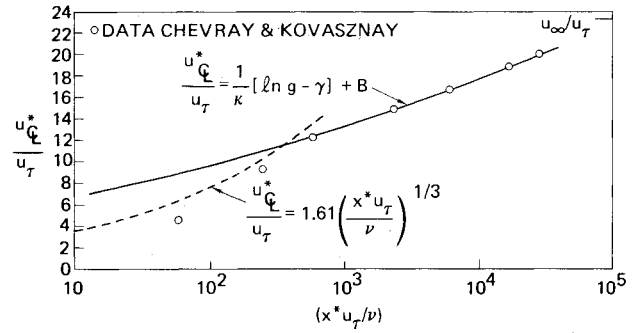

Fig. 4 Centerline velocity (semilogarithmic plot).

From Eq. (71) it is readily seen that the mean velocity of the inner wake solution always approaches the upstream logarithmic law of the wall, for large values of $y^* u_\tau/\nu$. The experimental data shown in Fig. 3 demonstrate that this asymptotic behavior is approximately valid for the velocity profiles at wake locations $x^* = 5$ cm ($x^* u_\tau/\nu = 586$) and $x^* = 20$ cm ($x^* u_\tau/\nu = 2342$) and begins to deviate from the logarithmic form at $x^* = 50$ cm ($x^* u_\tau/\nu = 5855$), about ten boundary-layer thicknesses from the trailing edge. One would thus expect that the region II inner wake solution would become invalid at further downstream stations.

The development of the theoretical [Eqs. (22) and (53)] and experimental centerline wake velocity with downstream distance is shown in Fig. 4. Note that very close to the trailing edge ($x^* u_\tau/\nu < 300$), the two measured centerline velocity data points tend to follow the equivalent laminar Goldstein solution given by Eq. (22). For $x^* u_\tau/\nu > 300$, the data follows the first-order centerline logarithmic velocity solution [Eq. (53)] quite closely. The good agreement up to distances $x^* u_\tau/\nu \approx 3 \times 10^4$ is rather surprising, since for values of $x^* u_\tau/\nu > 5 \times 10^3$, the outer logarithmic boundary condition for the inner wake solution is not satisfied, as noted in the preceding paragraph.†

In Ref. 10, as well as in the 1972 NASA Langley Conference on free turbulent flows,[3] (for which this flat plate wake flow problem was treated numerically by turbulent modelers), the wake centerline velocity is always shown scaled

†Andreopoulos[14] recently reported hot-wire measurements of the turbulent near wake of a symmetric thin airfoil which show centerline velocity data closely following the logarithmic behavior of Chevray and Kovasznay.[10] Interestingly, it was stated by Andreopoulos that "there is no theoretical justification for the semilogarithmic relationship."

according to far-wake (region III) similarity scaling laws, $(u^*_\infty - u^*_\ell)/u^*_\infty \sim (x^*)^{-1/2}$. The present analysis shows that for distances of 10 to as much as perhaps 100 initial boundary layers downstream of the trailing edge, that the far wake scaling is inappropriate and should be replaced by the scaling given by Eq. (53) where the centerline velocity increases approximately logarithmically with downstream distance.

V. Induced Pressure Gradients near the Trailing Edge

The Goldstein solution for the vertical velocity v in region I of the near wake indicates the inner wake induced inflow to the outer layer, $v_{\text{outer}} \sim x^{-2/3}u(0,y)$ becomes singular at the trailing edge of the flat plate, $x=0$. Stewartson[12] and Messiter[13] have shown in the laminar case that such an inflow induces a pressure change in the outer potential flow, which is of the same order as v_{outer}. By allowing the pressure and outer boundary layer to couple in with the acceleration of the inner wake, Stewartson and Messiter were able to develop a rationale theory for viscous-inviscid interactions at the trailing edge which removed the singularity in v at $x=0$. The formalism for this interaction theory is now commonly referred to as the triple-deck theory [after Stewartson (1969)]. In this formalism, the lower deck asymptotically approaches the Goldstein inner layer solution when the axial distance is large compared to some pressure gradient length scale x^*_{PG}. The main deck which is inviscid but rotational in nature couples the streamline displacement generated by the inner wake to the pressure field of the upper deck, which is basically a potential flow.

The first step in developing the corresponding triple-deck formalism for the turbulent problem is to estimate the horizontal and vertical scale sizes for the lower and middle decks. To estimate the scale for pressure changes in the region I wake, we note from inviscid potential flow theory that the normalized outer pressure and outer vertical velocity [Eq. (30)] are of the same order,

$$\frac{P^*_{\text{outer}} - P_\infty}{\rho u^2_\infty} \sim \frac{v^*_{\text{outer}}}{u_\infty} \sim \left(\frac{x^* u_\tau}{\nu}\right)^{-2/3} \tag{72}$$

In the lower deck, the pressure gradient is as given by Eq. (72) and is of the order of the acceleration term in the axial momentum equation. For an axis velocity growing like the cube root of x [Eq. (22)], we find that the scale for pressure gradient effects is given by

$$\left(\frac{x^* u_\tau}{\nu}\right)_{\text{PG}} \sim \left[\frac{u_\tau}{u_\infty}\right]^{-3/2} \sim O(10^2) \tag{73}$$

In terms of plate length L,

$$x^*_{\text{PG}} = L/[R(u_\tau/u_\infty)^{5/2}] \tag{74}$$

The corresponding vertical height scale is estimated by equating the acceleration and diffusion terms in the lower deck yielding

$$y^*_{\text{PG}} = L/[R(u_\tau/u_\infty)^{3/2}] \tag{75}$$

Lighthill[13] obtained basically the same result as Eqs. (74) and (75) in his study of interacting supersonic boundary layers.‡ Note that for moderate Reynolds numbers and $u_\tau/u_\infty \approx 0.04$ the axial scale for region I pressure gradient interaction is a very small fraction of a plate length. This interaction scale is comparable with the distance for the transition from region I to region II wake development, $x^* u_\tau/\nu \sim 0(10^2)$, or about ten laminar sublayer thicknesses.

In region II one can also make an estimate for the pressure gradient length scale, provided that one assumes that the logarithmic solution for region II is carried back toward the trailing edge. For significant pressure gradient effects, the log of the axis scale parameter $g(x)$, given by Eq. (39), is estimated to be of the order

$$[\ell n g]_{\text{PG}} \sim O\left[\kappa \Big/ \left(\frac{u_\tau}{u_\infty}\right)^{1/2}\right] \tag{76}$$

Equation (74) indicates that pressure gradient effects should be confined to a region close to the trailing edge where $x^* u_\tau/\nu < 100$. Thus, pressure gradient effects will principally be confined to region I and can, for the most part, be neglected in region II as the data of Chevray and Kovasznay seem to substantiate.

VI. Concluding Remarks

The present analysis has pointed out the importance of the Goldstein region I inner wake development and the logarithmic inner wake development of region II, when one examines the near wake close to the trailing edge of a constant pressure flat plate flow with an initial turbulent boundary layer.

The solution for the two regions is, of course, not complete. The two regions should be joined by some sort of transitional solution in which the laminar and turbulent eddy diffusivities are of the same order. The behavior of other more complex mathematical expressions for the region II inner wake eddy diffusivity might be examined. However, the simplicity of the linear eddy diffusivity model solution perhaps would be lost. Further studies of the turbulent trailing-edge problem might undertake to give a more formal high Reynolds number asymptotic derivation of the major features developed here for the trailing-edge solution.

Finally, we should comment further on the results presented in Sec. V. The pressure interaction scaling near the trailing edge is only valid in the zero angle-of-attack case. When external pressure gradient effects from the outer inviscid flow become dominant, as for a flat plate or airfoil at angle of attack, it is clear that the scaling for inner wake development will be noticeably altered. The work of Melnik et al.[15] on the airfoil trailing-edge problem, at large angle of attack, produced a significant difference in scaling for trailing-edge and near-wake effects because of the "imposed" external pressure field. If one posed the airfoil near-wake problem for the case of a small angle of attack (α) with a cusped-type trailing edge, a formal analysis should merge with the present treatment as $\alpha \to 0$. Whether this is significant for the engineering problem of calculating viscous corrections to airfoil lift can be examined perhaps in future treatments of this problem for the case of a plate or wedge at finite angle of attack.

Acknowledgment

This study was initiated while the author was a Senior Research Fellow in the Dept. of Mathematics at University College, London. Financial support from the Science Research Council of Great Britain is gratefully acknowledged. I am indebted to Professor K. Stewartson for his insight, guidance, and interest during the development of this study.

References

[1] Goldstein, S., "Concerning Some Solutions of the Boundary Layer Equations in Hydrodynamics," *Proceedings of the Cambridge Philosophical Society*, Vol. 26, Pt. 1, 1930, pp. 3-30.

[2] Bradshaw, P., "Prediction of the Turbulent Near Wake of a Symmetrical Aerofoil," *AIAA Journal*, Vol. 8, Aug. 1970, pp. 1507-1508.

‡For low speed laminar flows, $u_\tau/u_\infty \sim 0(R^{-1/4})$, yielding $x^*_{\text{PG}} = 0(R^{-3/8})$, $y^*_{\text{PG}} = 0(R^{-5/8})$, which are the scales for Stewartson's[11] lower deck interaction solution for the corresponding laminar problem.

[3] *Free Turbulent Shear Flows, Volume I—Conference Proceedings, Volume II—Summary of Data,* NASA Langley Research Center, July 1972, NASA SP-321.

[4] Burgraff, O. R., "Comparative Study of Turbulence Models for Boundary Layers and Wakes," Aerospace Research Lab., TR-74-0031, March 1974.

[5] Coles, D., "The Law of the Wake in the Turbulent Boundary Layer," *Journal of Fluid Mechanics*, Vol. 1, Pt. 2, July 1956, p. 191.

[6] Melnik, R. E., personal communication, 1979.

[7] Robinson, J. L., "Similarity Solutions in Several Turbulent Shear Flows," NPL Rept. 1242, 1967.

[8] Townsend, A. A., "Self-Preserving Flow Inside a Turbulent Boundary Layer," *Journal of Fluid Mechanics*, Vol. 22, Pt. 4, 1965, pp. 773-797.

[9] Townsend, A. A., "The Flow in a Turbulent Boundary Layer After a Change in Surface Roughness," *Journal of Fluid Mechanics*, Vol 26, Pt. 2, 1966, pp. 255-266.

[10] Chevray, R. and Kovasznay, L.S.B., "Turbulent Measurements in the Wake of a Thin Flat Plate," *AIAA Journal*, Vol. 7, Aug. 1969, pp. 1641-1643.

[11] Stewartson, K., "On the Flow Near the Trailing Edge of a Flat Plate," *Mathematika*, Vol. 16, 1969, pp. 106-121.

[12] Messiter, A. F., "Boundary Layer Flow Near the Trailing Edge of a Flat Plate," *SIAM Journal of Applied Mathematics*, Vol. 18, Jan. 1970, pp. 241-257.

[13] Lighthill, M. J., "On Boundary Layers and Upstream Influence, Pt. II. Supersonic Flows Without Separation," *Proceedings of the Royal Society of London, Part A*, Vol. 217, 1953, p. 478.

[14] Andreopoulos, J., "Turbulent Near Wakes of a Thin Aerofoil," Paper presented at the Second Symposium on Turbulent Shear Flows at Imperial College, London, July 1979.

[15] Melnik, R. E., Chow, R., and Mead, H. R., "Theory of Viscous Transonic Flow Over an Airfoil at High Reynolds Number," AIAA Paper 77-680, June 1977.